A comparative examination of steam-powered screw motors for specific installation conditions[1)]

Dipl.-Ing. Jan Hütker, TU-Dortmund, Chair of Fluidics
Univ. Prof. Dr.-Ing. Andreas Brümmer, TU-Dortmund, Chair of Fluidics

Abstract

The examination of the influence of the geometric machine parameters on the thermodynamic operating behaviour of steam-powered screw motors for specific installation conditions depends to a great extent on defining the design criteria. Although research carried out in the past, under the restriction of constant theoretical mass flows, permitted basic insights into the main loss mechanisms in steam screw motors, these results were only of limited validity for the design of the machine geometry for constant speed installation conditions. The variation and examination of the energy-based influence of the geometrical parameters, under the boundary condition of constant mass flows, takes into account the sensitive nature of the volumetric efficiency of steam screw motors, and makes it possible to design machines for specific installation conditions.

1. Introduction

Screw machines employed as motors, utilising the expansion of vaporous working fluids, are found in decentralised energy systems in the low and medium performance ranges. In these applications, the high efficiency and good performance under part-load conditions over a wide load range are mainly responsible for the energy-based advantages of the screw motor compared with other mechanical concepts. Low requirements for the working medium make it possible to use, for example, the expansion of normal steam in any non-critical form. This opens up applications for screw motors which are not suitable for turbines.

The influence of the geometrical machine parameters on the thermodynamic operating behaviour of steam-powered screw motors has already been intensively examined and assessed in quantitative terms. The geometry-dependent, principal loss mechanisms, are composed mainly of choke effects and gap losses during the charging phase. The quantitative evaluation of the energy conversion efficiency in terms of internal power, isentropic efficiency, or in terms of machine-specific performance data, has always been carried out under the restriction of a constant theoretical mass flow. The theoretical mass flow, considered as the product of the chamber volume at the theoretical start of expansion, the compression as a function of the values at the motor inlet, the tooth count and the rotor speed, thus depends – along with the entry conditions – only on the known machine geometry and the rotor speed, but not on the motor parameters. However, for the development and examination of screw motors for specific installation conditions the theoretical mass flow is unsuitable as a design criterion. This is because the sensitivity of volumetric efficiency to the necessary mass flow for optimal energy conversion often differs considerably from the theoretical mass flow. Within the framework of this article, motor variants for specific installation conditions with differing geometrical parameters will

[1)] **This work is supported by the BMBF (Bundesministerium für Bildung und Forschung)**

be examined. Geometrical similarity is assumed, and the machines will be scaled at identical transported mass flows as a design criterion. The influence of the selected boundary condition on the desired geometrical machine parameters is clarified here mainly through an examination of the volumetric efficiency. The description of the loss mechanisms is carried out using geometrical and installation-specific performance figures.

2. Loss mechanisms

The description of loss mechanisms during the working cycle of a steam-powered screw motor is carried out on a typical machine, selected with reference to the indicator diagram in **Fig.1**.

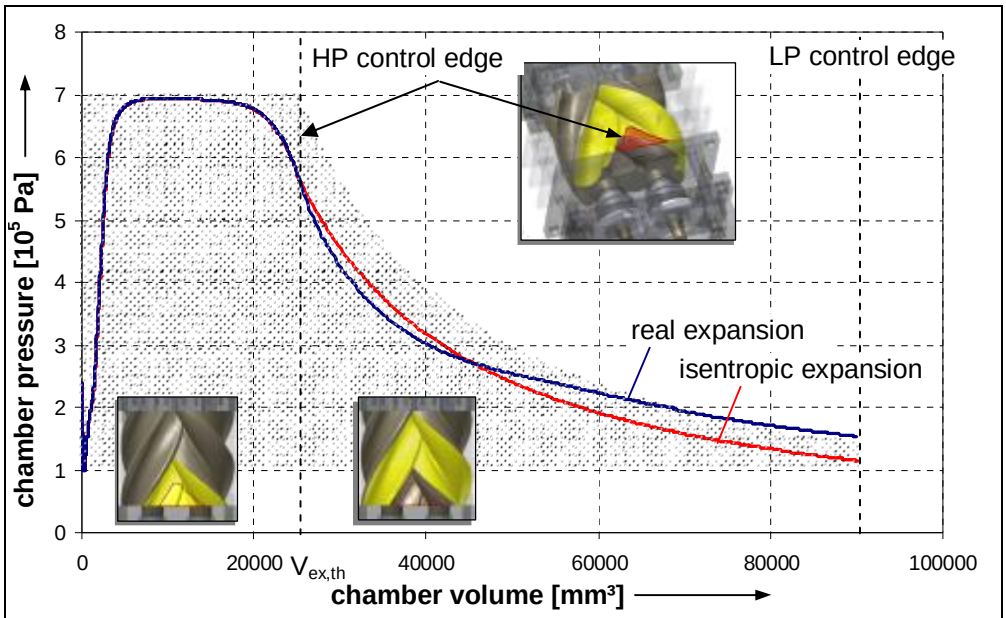

Fig.1: Chamber pressure progression dependent on chamber volume with real and isentropic charging / expansion phase.

As the inlet opening has a small area at the start of the working cycle, resulting in a high choking effect, maximum chamber pressure is not established instantaneously, but builds up gradually as the rotor turns. The pressure difference between the entry pressure p_E and the chamber pressure p_C is characteristic for the charging phase. This pressure difference results on the one hand from choking losses during inflow and on the other hand from gap mass flows. A further characteristic of the real charging procedure is the start of expansion before the high pressure side control edge is reached. The pressure gradient at chamber volume V_{Ex} already resembles that at of the first expansion phase as the control edge is reached from $V_{Ex,th}$. on. The reason for the early start of real expansion is mainly the combination of continually rising chamber volume and reduction in the area of the inlet opening towards the end of the charging phase. This early start is an inherent part of the system and it also occurs in an ideal simulation, ignoring choking and gap loss factors which result from flow obstruction in the inlet cross-section.

At the start of the expansion phase the operating behaviour of the screw motor is significantly influenced by the gap mass flows. In order to evaluate the influence of these flows on the energy conversion efficiency of the motor, we need to distinguish between mass flows out of the working chamber under examination and flows into it via the gap connections. Compared with isentropic expansion, the real pressure gradient during expansion is steeper at the theoretical start of expansion. The reason for this is the predominant share of mass flows out of the working chamber compared with flows into it. As the rotation angle increases, real and isentropic chamber pressures continue to converge, until, in the second phase of expansion, pressures for the real process attain higher values than those in the isentropic expansion phase. The flatter pressure curve of the real process in this area is a result of mass flows into the working chamber from the following chambers. These flows do not go direct to the low pressure side of the motor, but flow in part to the expanding chamber under examination, so that they apply work to the rotor flanks. The expansion phase ends when maximum chamber volume is attained. As a rule, at this rotation angle, the front tooth flanks cross the low pressure side control edges, and pressure equalisation takes place between the working fluid and the low pressure side volume (shown isochorically in Fig. 1). In the following, in order to represent the expulsion process, an idealised isochoric pressure equalisation process between the chamber pressure and the low pressure side ambient installation pressure is assumed. The influence of the pressure difference between the end of expansion and ambient back pressure is considered below, during examination of the internal volume ratios, in connection with “over and under-expansion”.

3. Performance data for the evaluation of screw motors

In order to evaluate the energy conversion efficiency of screw motors with varying geometrical parameters, performance figures and boundary conditions have to be laid down, at values for which the various different motors are comparable. Although a screw motor functions in basically the same way as a screw compressor rotating the opposite direction, both the definition of the boundary conditions and the physical description of the processes in the working chambers are more complex than in the case of screw compressors. In the following, performance figures will be defined and applied which permit both the assessment of differing rotor geometries, and the energy-based consideration of differing motor variants.

For a quantitative assessment of the gap situation and the configuration of the inlet area, the gap and inlet area operating data will be defined below. In contrast to flow rate and volumetric efficiency, the two previous sets of figures describe the geometric characteristics of the screw motor, and are independent of an energy-based examination of the whole working cycle.

The gap operating data relate the fluid mass $m_{G,fill}$ to the theoretical fluid mass $m_{Ex,th}$ at the start of expansion:

$$\Pi_G = \frac{m_{G,fill}}{m_{Ex,th}} \qquad \text{(Equation 1)}$$

The fluid mass $m_{G,fill}$ is the mass which, in the rotation angle area for charging between $\alpha_{fillbegin}$ and $\alpha_{Ex,th}$, flows out of the working chamber through the time-dependent gap area of the chamber to be charged A_G (t). For the gap flow, a supercritical decompression, reaching the speed of sound in the narrowest cross-section, is assumed

$$\Pi_G = \frac{\int_{\alpha_{fillbegin}}^{\alpha_{Ex,th}} A_G(t)\ \frac{1}{\omega}\,d\alpha \cdot \left(\frac{2}{\kappa_E+1}\right)^{\frac{1}{\kappa_E-1}} \cdot \frac{p_E}{R \cdot T_E}\sqrt{\frac{2\cdot\kappa_E}{\kappa_E+1}\cdot R \cdot T_E}}{V_{Ex,th}\cdot\rho_E} \qquad \text{(Equation 2)}$$

The calculation is based on the model of a constant and isentropic gap flow through the narrowest cross-section, with negligible flow speeds before the entrance. If we assume that there is a flow blockage, the leakage becomes a function of the entry parameters (temperature and pressure), and the time (r.p.m.), and of the geometrical and time-dependent gap area. The theoretical mass can be computed from the chamber volume at the theoretical start of expansion, and the entry compression. It therefore depends on the entry parameters and the geometry of the screw motor.

The entry area operating data relates the mean fictive inflow speed to the speed of sound $a_E = f(p_E, T_E)$:

$$\Pi_{IA} = \frac{\bar{c}_{E,f}}{a_E} = \frac{\overline{\left(\frac{\dot{V}_C(t)}{A_{IA}(t)}\right)}}{a_E} \qquad \text{(Equation 3)}$$

The fictive inflow speed already used by Huster and Kauder is computed on the basis of the change in the chamber volume $\dot{V}_C(t)$ over time, and the inlet area A_{IA} (t). This means that the relationship between the mean fictive inflow speed and the speed of sound can be interpreted as a kind of mean fictive Mach number in the entry cross-section. Analogous to the gap operating data, the entry area data is only dependent on the geometry and the entry parameters. A motor with low entry area values is desirable, as this corresponds with a long charging phase and a large entry area.

4. Boundary conditions

In the following variation calculations, the parameter combination of entry pressure p_E and entry temperature ϑ_E are set as fixed boundary conditions for the screw motor, along with the mass flow at a constant ambient back pressure of $p_B = 10^5$ Pa. Although the variation options cover a broad, technically reasonable range, the fixing of the boundary conditions is not random, but is based on installation conditions of the type which occur in industrial applications with low mass flows.

- working medium: steam
- entry pressure $p_E = 7\cdot10^5$ Pa
- entry temperature ϑ_E = 350 °C
- mass flow = 0,1 kg·s^{-1}

In the following variation calculations, the mass flow is considered both as a theoretical reference value and as a real flow rate. The theoretical mass flow depends only on the machine geometry and the rotor speed, but not on the motor performance values, and is calculated via the following equation:

$$\dot{m}_{th} = V_{Ex,th} \cdot \rho_E \cdot z_{MR} \cdot n_{MR} = \frac{V_{max}}{v_i} \cdot \rho(p_E, T_E) \cdot z_{MR} \cdot n_{MR} \qquad \text{(Equation 4)}$$

The mass flow of the installation corresponds to the mass flow actually transported, and it depends not only on the machine geometry and the entry condition, but also on physical loss mechanisms. Along with the constant installation parameters, a number of other boundary conditions also need to be defined. These boundary conditions are laid down as the circumferential velocity at the tip circle of the rotors, and the mean gap height. For the variation in the rotor geometry, the male rotor circumferential velocity is set at u_{MR} = 80 $m \cdot s^{-1}$ as a constant. Gap heights of h_G = 0,1 mm for the entire machine are adopted as a constant.

5. Modelling and computing

The variation calculations were carried out in two independent computation steps: a geometrical abstraction and an energy-based examination. The basis of the geometrical abstraction of a screw motor is the analytical treatment of the rotor meshing. The objective of this calculation is to determine the volume curve, and to determine the inlet and outlet areas and the gap areas as a function of the male rotor angle, with preset geometrical parameters (z_{MR}, z_{MR}, φ_{MR}, L/D und v_i). The results of the geometrical abstraction are the basis for an energy-based examination of the operating behaviour of the motor.

The computing program for the energy-based machine analysis is based mainly on mass and energy conservation. Basically, by means of a balancing process, changes in the condition of the vaporous working fluid are ascertained numerically, so that the operating behaviour of the machine can be represented. This allows changes in condition in the form of rotation angle dependent volume changes, and gap mass flows in and out of the working chamber, to be taken into account. The computational basis for process changes in the working fluid is represented with reference to the flow velocity by a zero-dimensional chamber model, which permits, in principle, the simulation of screw motors with any range of geometrical parameters.

6. Geometrical variations

The following design for the geometrical parameters of the screw motor comprises variation in the internal volume ratios, the wrap angles, and the length-diameter ratios. As a starting point for the variation calculations, a tooth count combination of four male rotor teeth (z_{MR} = 4) and six female rotor teeth (z_{MR} = 6) was selected, which represents a compromise between low integral gap areas and a sufficiently large rotation angle area for chamber charging.

6.1. Variation of the internal volume ratio

The internal volume ratio is independent of the rotor geometry, and is configured exclusively via the position of the control edges in the motor housing. According to the official definition, the internal volume ratio of a screw motor is the result of the relationship between the maximum chamber volume at the end of expansion V_{max} and the chamber volume at the theoretical start of expansion $V_{Ex,th}$:

$$v_i = \frac{V_{max}}{V_{Ex,th}} \qquad \text{(Equation 5)}$$

Variation of the internal volume ratio of a screw machine takes place, in the case of deployment as a motor, by adjusting the position of the high pressure side control edges. With constant geometric rotor parameters, an increase in the internal volume ratio causes an adjustment of the control edges towards smaller rotor rotation angles, which results in a decrease in chamber volume at the start of expansion. Therefore, when varying the internal volume ratio, a requirement for constant mass flow in combination with constant male rotor circumferential velocity constitutes a significant restriction in machine dimensions.

The geometrical and energy-based effects of a variation in the internal volume ratio for machines with a wrap angle φ_{MR} = 300° and a length-diameter ratio L/D = 1,4 are illustrated below (**Fig. 2** and **Fig. 3**).

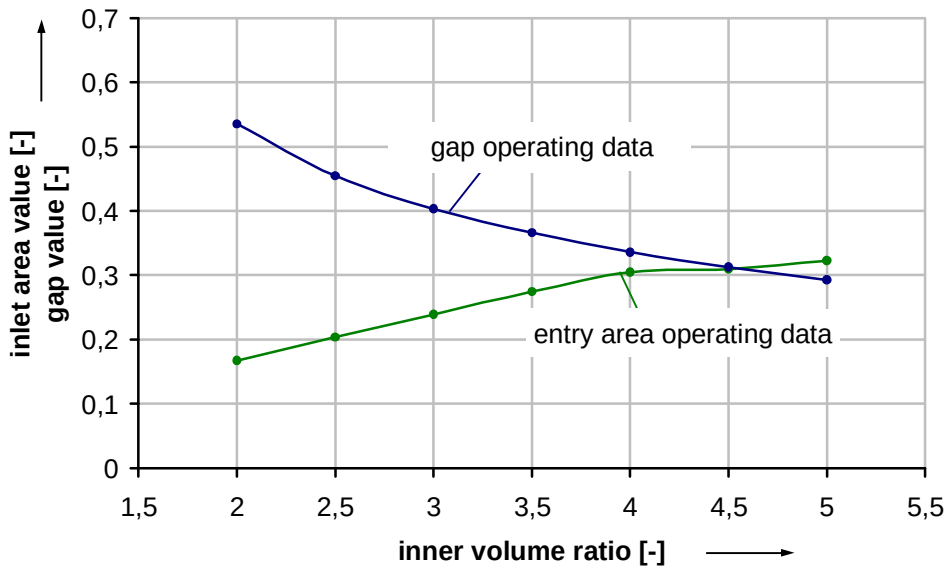

Fig 2: Entry area operating data and gap operating data as a function of the internal volume ratio for constant mass flow in the machine.

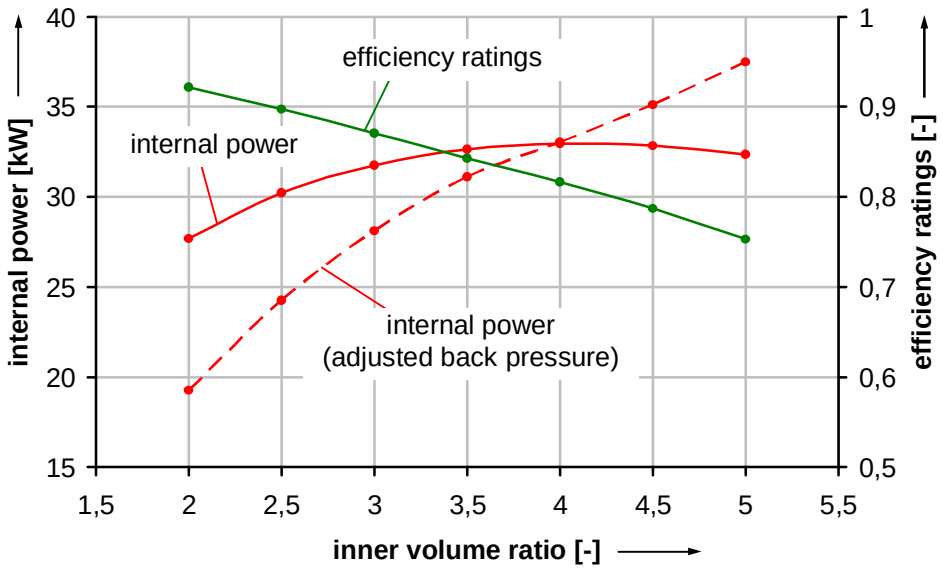

Fig 3: Internal isentropic efficiency rating and internal power at constant ambient back pressure and adapted operation as a function of the internal volume ratio.

At low internal volume ratios, the gap operating figures achieve maximum values, and the inlet area figures achieve minimal values. In this parameter area, the favourable inlet area data can be explained in terms of late arrival of the high pressure side control edge and the correspondingly large rotation angle area which is available for charging the working chamber, along with a large maximum inlet area. However, both the long charging time and the unfavourable gap situation lead to high mass flows through the gaps.

As internal volume ratios increase, the gap operating figures decrease and the inlet figures increase, which results mainly from the shorter rotation angle area available for the charging process. The dominant influence of inlet choking on the energy conversion efficiency of screw machines can be explained in terms of the dependence of the internal isentropic efficiency rating[2)] on the internal volume ratio. The efficiency rating drops virtually in a straight line as the internal volume ratio rises, in spite of an improving gap situation, as a consequence of the deteriorating charging situation . On the other hand, internal power is affected primarily by the relationship between chamber pressure at the end of expansion and ambient back pressure. If the internal volume ratio selected is too low, this leads to chamber pressure above the low pressure side ambient pressure, and this ‘under-expansion’ results in an idealised isochoric ‘after-expansion’ of the working fluid as the low pressure control edges are passed. Part of the theoretically available exergy of the fluid thus remains unused because the expansion phase is too short. Maximum internal power is produced in ‘adapted operation’. In this case there is no difference between the chamber pressure at the end of expansion and the low pressure side ambient pressure. As internal volume ratios continue to rise, chamber pressure drops below ambient pressure during expansion, and internal power falls away sharply. The ‘over-expanded’ fluid

[2)] The internal isentropic efficiency rating corresponds to the working area ratio of the loss-impaired motor when compared with the geometrically similar motor without losses (isobaric charging up to $V_{ex,th}$ and isentropic expansion up to V_{max}

mass is compressed in idealised isochoric form by the working fluid flowing back from the low pressure port before it is expelled. As soon as the chamber pressure falls below ambient pressure on the low pressure side, the effective work produced during the expansion of the fluid is over-compensated for by the work necessary for expulsion.

Fig. 3 shows the dependence of the internal power on the internal volume ratio for adjusted low pressure side back pressure. As examined here, the steam-powered screw motor always works in adjusted mode, and shows increasing internal power across the whole parameter range. This is a consequence of the increasing working area as the internal volume ratio rises, but it also shows – through the declining dependence of internal power on the internal volume ratio – the influence of the unfavourable inlet area situation with large internal volume ratios. An examination of the influence of the internal volume ratio on the thermodynamic operating behaviour of steam-powered screw motor reveals similar tendencies both for the mass flow in the installation and the theoretical mass flow as a design criterion. It was decided not to include the calculation results for machines with constant theoretical mass flows, as for this design boundary condition, tool, steam screw machines with an internal volume ratio which permits adjusted operation achieve the highest internal power results.

6.2. Variation of the wrap angle

In order to examine and evaluate the effects of varying the wrap angle on the energy conversion efficiency of screw motors, both for the design criterion of constant theoretical mass flow and for constant installation mass flow, a number of pairs of rotors are varied so that only the wrap angle changes. The length-diameter ratios and the internal volume ratios of all rotor pairs remain constant. Varying the wrap angle influences both the gap situation and the geometry of the inlet area. For the quantitative description of the geometrical effects of the machine variations, an entry area value Π_{IA} and a gap value Π_G are used. The dependence of both values and that of the volumetric efficiency on the wrap angle, plus the internal power and the internal isentropic efficiency rating as a function of the wrap angle, are represented in **Fig. 4** and **Fig. 5** for screw motors with an internal volume ratio of $v_i = 3,5$ and a length-diameter ratio L/D = 1,4, for the design criterion of constant theoretical mass flow. The geometry of motor variants with small wrap angles is characterised by a favourable gap situation and unfavourable inlet area geometry. For these motor variants both the internal isentropic efficiency rating and the internal power rating only attain minimal values. As the wrap angle increases, the efficiency rating and the internal power rise digressively, which can be explained in terms of integrally reducing dissipation. With reference to the entry area and gap operating datas, the most important factor is the improved energy conversion efficiency which is brought about by better inlet geometry as a result of increasing wrap angles. This factor plays a greater role than the deteriorating gap situation. If we consider the design criterion of constant theoretical mass flow, the favourable characteristics, from an energy conversion point of view, of motors with large wrap angles, are present for all length-diameter ratios and internal volume ratios examined. The volumetric efficiency of the steam-powered screw motors under examination rises as the wrap angle increases from $\lambda_L \approx 0,95$ to $\lambda_L \approx 1,2$ upwards.

Concerning constant installation conditions, machine versions with large wrap angles show a corresponding installation mass flow, which lies about 20 % above the theoretical mass flow set as a design criterion.

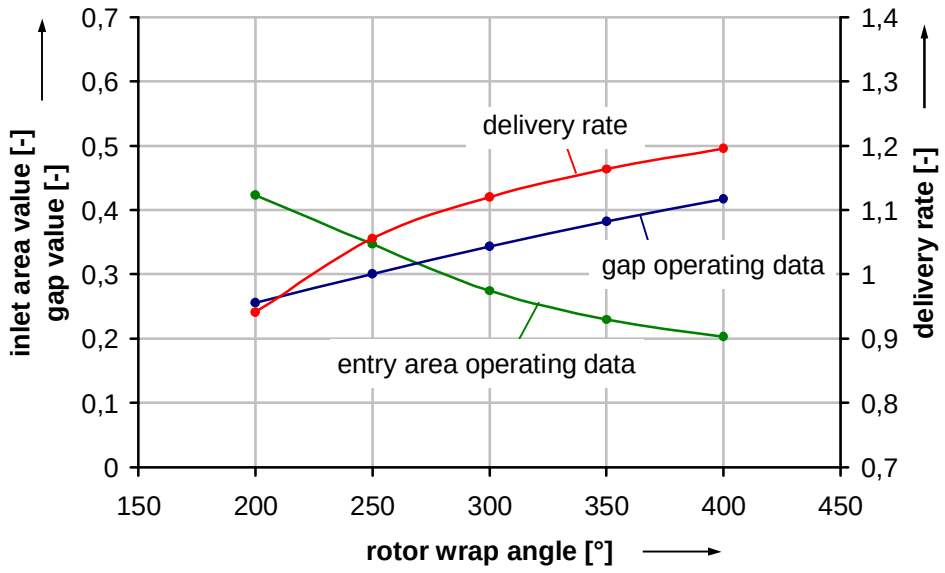

Fig. 4: Entry area operating data, gap operating datas and delivery rate as a function of the wrap angle for constant theoretical mass flow

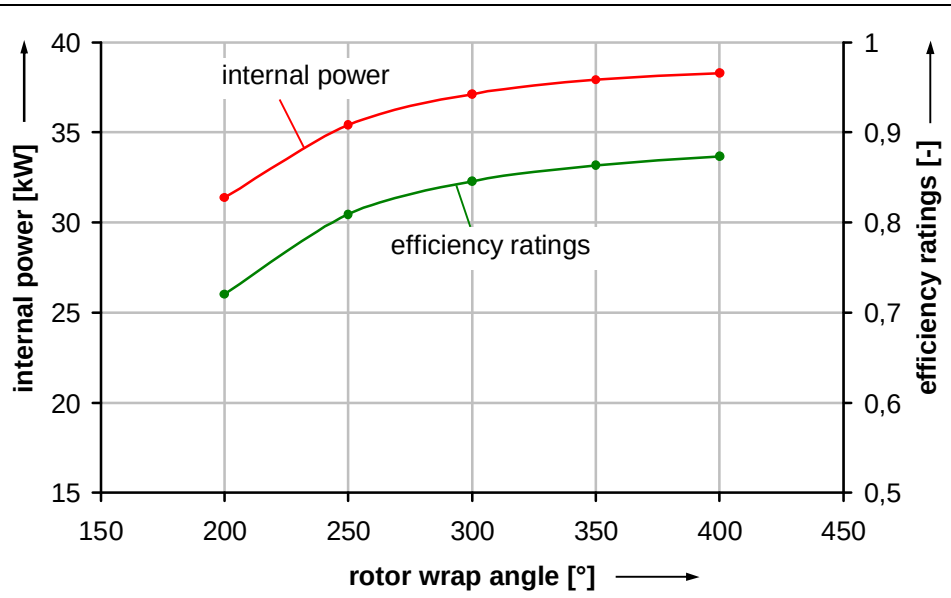

Fig. 5: Internal isentropic efficiency rating and internal power as a function of the wrap angle for constant theoretical mass flow

The effects of geometrical scaling of the motors on a constant installation mass flow are outlined in **Fig. 6** and **Fig. 7** for the machine parameters already utilised.

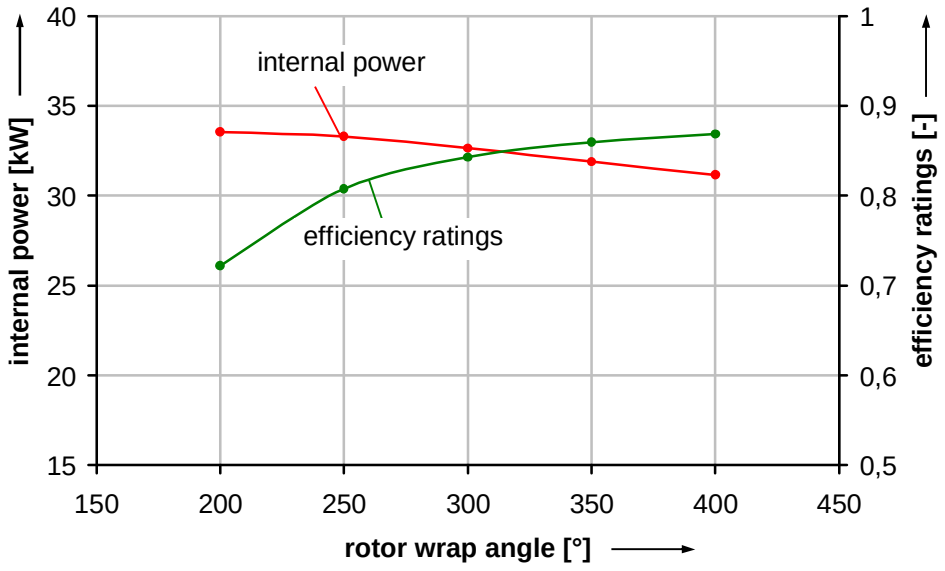

Fig. 6: Internal isentropic efficiency rating and internal power as a function of the wrap angle for constant installation mass flow

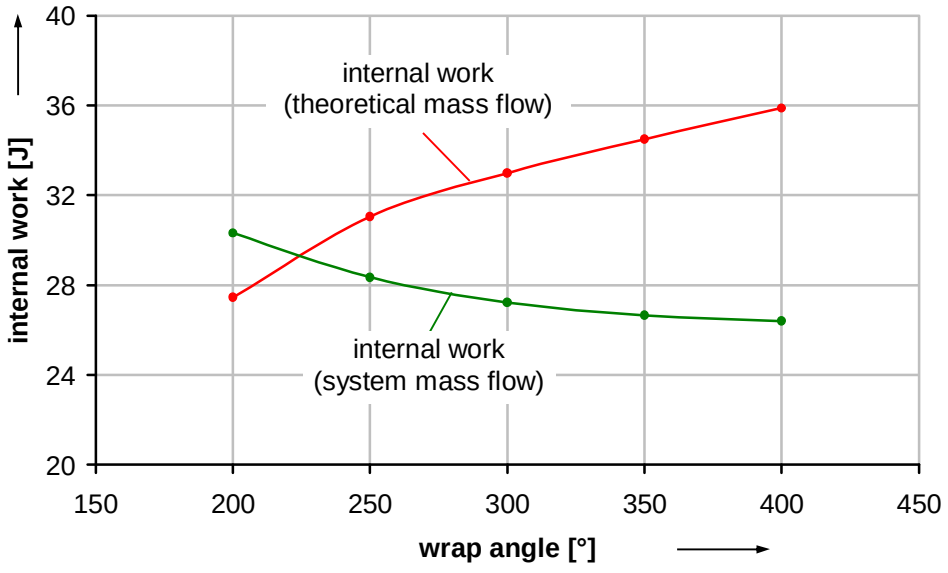

Fig. 7: Internal work for constant theoretical and system mass flow as a function of the wrap angle

While for a configuration based on theoretical mass flow the largest possible wrap angle emerges as reasonable from an energy point of view, constant installation mass flow machines with small wrap

angles produce the highest internal power. Although, as the qualitative interrelation of the geometric performance data (not covered here) and the internal isentropic efficiency remain unchanged, this state of affairs appears paradoxical, this shift in the internal power data can be explained via the scaling of the machine. In the large wrap angle area, the geometrical reduction in the size of the machine, a consequence of scaling down, results in a reduction in chamber volume. The energy-based influence of the reduction in volume is clarified by a computation of the internal work by means of the closed ring integral $W_i = \oint pdV$ and accordingly the internal power $P_i = \oint pdV \cdot z_{MR} \cdot n$. The reduction in the working area for motors with a large wrap angle is mainly responsible for the lower internal power at constant installation mass flows. The influence of rotor speed changes on internal power, also caused by scaling, is limited compared with the contribution to internal work. As far as constant installation parameters are concerned, it would appear that advocating large wrap angles, which would be the consequence of setting constant theoretical mass flow as a criterion, is not to be recommended.

6.3. Varying the length-diameter ratio

Along with the tooth count and the wrap angle, the length-diameter ratio is the third parameter which describes the rotor geometry. The variation area discussed below covers the range from length-diameter ratios L/D = 1,0 – 2,0. Analogous to the wrap angle, the length-diameter ratio influences both the total gap situation and the geometry of the inlet area of a steam-powered screw motor.

In **Fig. 8** and **Fig. 9**, for the design criterion of constant theoretical mass flow, both geometrical values, volumetric efficiency, the internal isentropic efficiency rating and internal power for an internal volume ratio of $v_i = 3,5$ and a wrap angle of $\varphi = 300°$ are represented.

In the area of small length-diameter ratios, the gap operating datas attain maximum ratings, and the entry area operating datas attain minimum ratings. As the length-diameter ratio increases, the growing entry area operating data is responsible for deteriorating geometrical characteristics in that area, while the reducing gap operating data exercises a positive influence on the gap situation. The effects of a rising length-diameter ratio on the inlet situation are qualitatively comparable with the influence of a reducing wrap angle at constant theoretical mass flow. Both the maximum value of the inlet area and the charging times decline as the length-diameter ratio falls, and are responsible for the high entry area operating datas in this parameter area. On the other hand, the reduced charging times have a favourable effect on the gap operating datas. As the length-diameter ratio increases, charging times and decreasing integral gap areas also contribute to the decline in this value. Both the internal isentropic efficiency rating and internal power attain maximum values at low length-diameter ratios, which, analogous to varying the wrap angle at constant theoretical mass flow, can be attributed to the predominant role of choking losses during charging compared with gap losses. The differences in volumetric efficiency from $\lambda_L \approx 1,18$ at small length-diameter ratios to $\lambda_L \approx 1,09$ at large length-diameter ratios are much smaller than is the case with wrap angle variation. Accordingly, scaling at

constant installation mass flow results in downsizing the machine across the entire parameter range under consideration. Machines with a small length-diameter ratio are the most seriously affected.

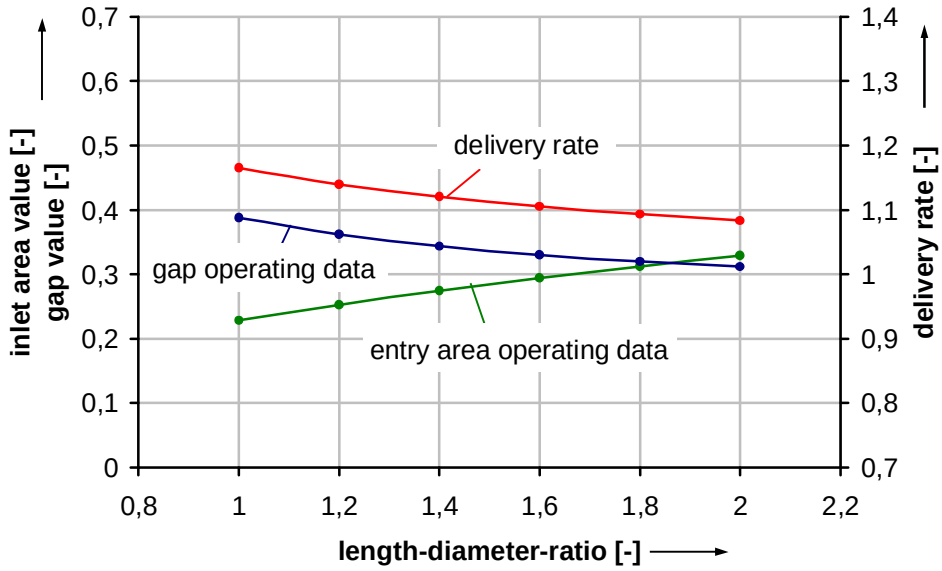

Fig. 8: Entry area operating data, gap operating data and delivery rate as a function of the length-diameter ratio for constant theoretical mass flow

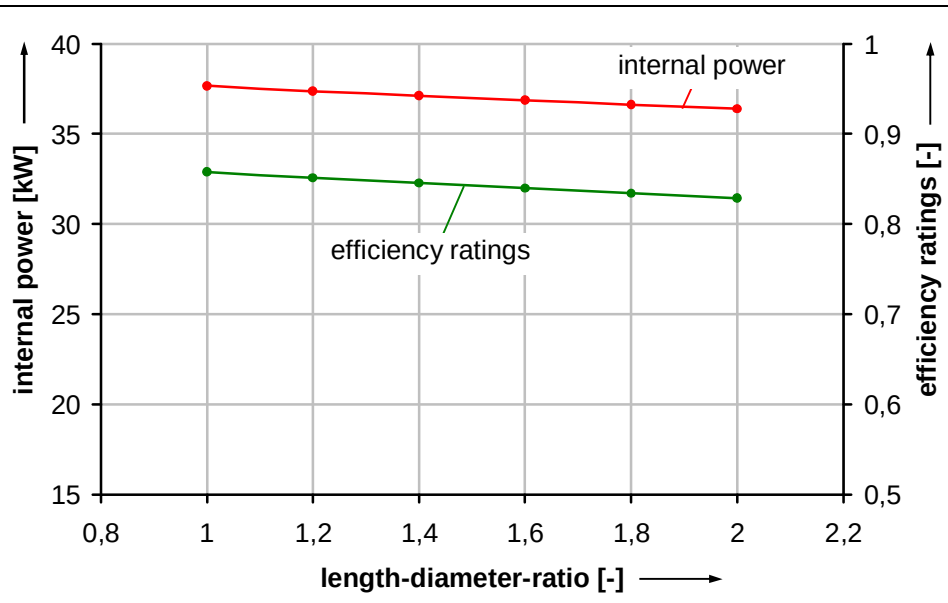

Fig. 9: Internal isentropic efficiency rating and internal power as a function of the length-diameter ration for constant theoretical mass flow

The energy figures for the scaled machines are represented in **Fig. 10** and **Fig. 11** as a function of the length-diameter ratio. As has been established for wrap angle variation, for length-diameter ratios, too,

scaling under constant installation conditions has no qualitative effect on geometrical performance values or isentropic efficiency rating.

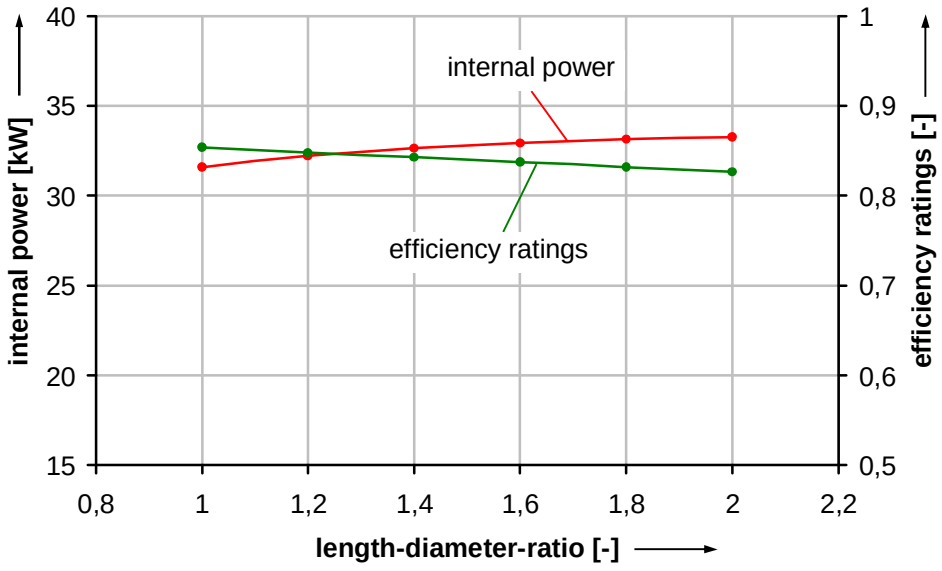

Fig. 10: Internal isentropic efficiency rating and internal power as a function of the length-diameter for constant installation mass flow

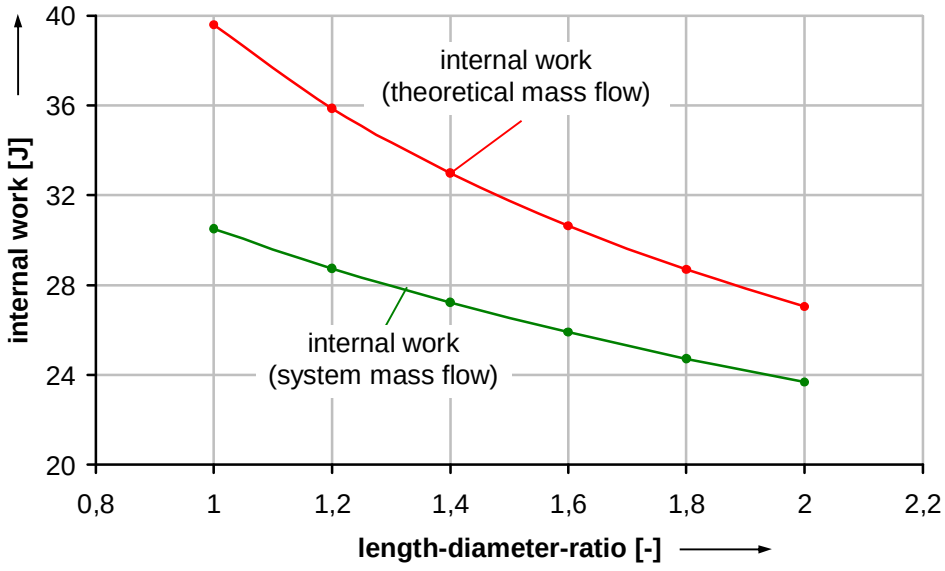

Fig. 11: Internal work as a function of the length-diameter ration for constant installation mass flow and theoretical mass flow

Scaling down entails a decrease in internal work across the whole range of variation. This decrease is most obvious in the case of small length-diameter ratios for machines with high volumetric efficiency.

However, internal work continues to attain maximum values at small length-diameter ratios. The rise in internal power as length-diameter ratios increase can not therefore be attributed to the enclosed working area of the thermodynamic cycle. It depends rather on the rise in rotor speed as a consequence of decreasing rotor diameter at high length-diameter ratios. While rotor speed changes played a minor role when the wrap angle was varied, for the machine examined in Fig. 10 and Fig. 11, across the range from n(L/D = 1,0) = 259 s^{-1} to n(L/D = 2,0) = 351 s^{-1} there was an increase of 35,5 % in rotor speed effect as the length-diameter ratio was varied. This explains the high internal power in the case of large length-diameter ratios.

For the used boundary conditions, the geometric parameters of the steam-powered screw motor are set to an internal volume ratio vi = 3,8, a wrap angle φ_{MR} = 300° and a length-diameter ratio L/D = 1,4. The chosen values are in case of the internal volume ratio and the wrap angle just a matter of the energetic analyses. The selected length-diameter ratio is a compromise between appropriate available space for bearings and packings on the one hand and good internal power on the other hand.

[1] Kliem, B.: Die Expansion von Naßdampf in Schraubenmotoren zur Nutzung von Abwärme - Ein Beitrag zur Auslegung von Zweiphasenschraubenmotoren. Dissertation, TU - Dortmund (2004)

[2] von Unwerth, T.: Experimentelle Verifikation eines Simulationssystems für eine GASSCREW. Dissertation, TU – Dortmund, (2002)

[3] Zellermann, R.: Optimierung von Schraubenmotoren mit Flüssigkeitseinspritzung. Dissertation, TU – Dortmund, (1996)

[4] Fost, C.: Ein Beitrag zur Verbesserung der Kammerfüllung von Schraubenmotoren. Dissertation, TU – Dortmund, (2003)

[5] Huster, A.: Untersuchung des instationären Füllvorgangs bei Schraubenmotoren. Dissertation, TU – Dortmund, (1998)

Symbol	Dimension	Meaning
a	$m\ s^{-1}$	speed of sound
A	m^2	Area
c	$m\ s^{-1}$	flow speed
D	M	diameter
h	M	gap height
l	M	length
$\dot{m}$	$Kg\ s^{-1}$	mass flow
n	s^{-1}	r.p.m
p	Pa	pressure
P	W	power/performance
R	$J\ kg^{-1}\ K^{-1}$	gas constant
t	S	time
T	K	temperature
u	$m\ s^{-1}$	rim speed
V	m^3	volume
$\dot{V}$	$m^3\ s^{-1}$	volume flow
W	$Kg\ m^2\ s^{-2}$	work, working area
v_i	-	internal volume ratio
z	-	tooth count

Symbol	Dimension	Meaning
°	Grad	rotation angle
η	-	efficiency rating
κ	-	isentropic exponent
Π_{IA}	-	entry area operating
Π_G	-	gap operating data
ρ	$kg\ m^{-3}$	density
φ	Grad	wrap angle
ϑ	°C	degrees Celsius

Symbol	Meaning
B	back pressure
C	chamber
E	entry/inlet
IA	inlet area
Ex	start of expansion
Ex,th	theoretical start of expansion
F	fictional
fill	charging
fillbegin	begin of filling / charging
Id	ideal
G	gap/clearance

A comparative examination of steam-powered screw motors for specific installation conditions[1)]

Dipl.-Ing. Jan Hütker, TU-Dortmund, Chair of Fluidics
Univ. Prof. Dr.-Ing. Andreas Brümmer, TU-Dortmund, Chair of Fluidics

Abstract

The examination of the influence of the geometric machine parameters on the thermodynamic operating behaviour of steam-powered screw motors for specific installation conditions depends to a great extent on defining the design criteria. Although research carried out in the past, under the restriction of constant theoretical mass flows, permitted basic insights into the main loss mechanisms in steam screw motors, these results were only of limited validity for the design of the machine geometry for constant speed installation conditions. The variation and examination of the energy-based influence of the geometrical parameters, under the boundary condition of constant mass flows, takes into account the sensitive nature of the volumetric efficiency of steam screw motors, and makes it possible to design machines for specific installation conditions.

1. Introduction

Screw machines employed as motors, utilising the expansion of vaporous working fluids, are found in decentralised energy systems in the low and medium performance ranges. In these applications, the high efficiency and good performance under part-load conditions over a wide load range are mainly responsible for the energy-based advantages of the screw motor compared with other mechanical concepts. Low requirements for the working medium make it possible to use, for example, the expansion of normal steam in any non-critical form. This opens up applications for screw motors which are not suitable for turbines.

The influence of the geometrical machine parameters on the thermodynamic operating behaviour of steam-powered screw motors has already been intensively examined and assessed in quantitative terms. The geometry-dependent, principal loss mechanisms, are composed mainly of choke effects and gap losses during the charging phase. The quantitative evaluation of the energy conversion efficiency in terms of internal power, isentropic efficiency, or in terms of machine-specific performance data, has always been carried out under the restriction of a constant theoretical mass flow. The theoretical mass flow, considered as the product of the chamber volume at the theoretical start of expansion, the compression as a function of the values at the motor inlet, the tooth count and the rotor speed, thus depends – along with the entry conditions – only on the known machine geometry and the rotor speed, but not on the motor parameters. However, for the development and examination of screw motors for specific installation conditions the theoretical mass flow is unsuitable as a design criterion. This is because the sensitivity of volumetric efficiency to the necessary mass flow for optimal energy conversion often differs considerably from the theoretical mass flow. Within the framework of this article, motor variants for specific installation conditions with differing geometrical parameters will

[1)] **This work is supported by the BMBF (Bundesministerium für Bildung und Forschung)**

be examined. Geometrical similarity is assumed, and the machines will be scaled at identical transported mass flows as a design criterion. The influence of the selected boundary condition on the desired geometrical machine parameters is clarified here mainly through an examination of the volumetric efficiency. The description of the loss mechanisms is carried out using geometrical and installation-specific performance figures.

2. Loss mechanisms

The description of loss mechanisms during the working cycle of a steam-powered screw motor is carried out on a typical machine, selected with reference to the indicator diagram in **Fig.1**.

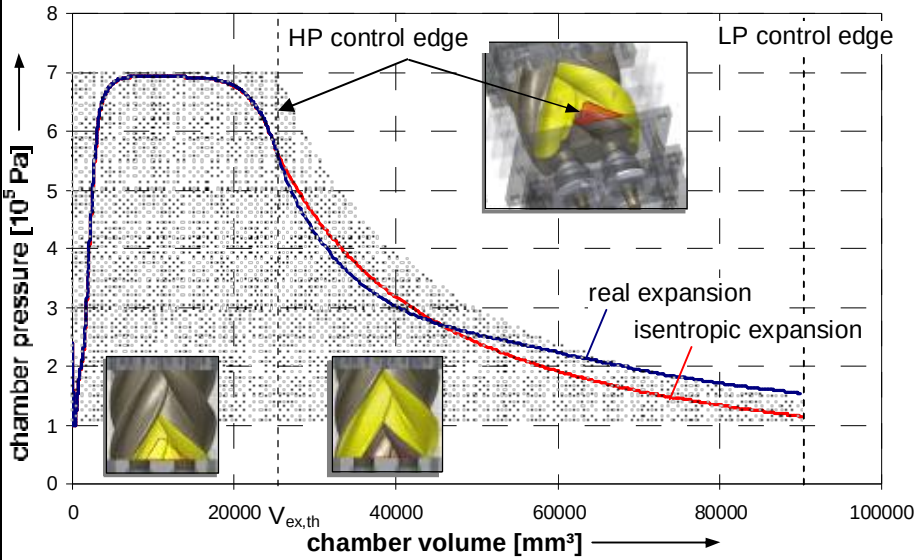

Fig.1: Chamber pressure progression dependent on chamber volume with real and isentropic charging / expansion phase.

As the inlet opening has a small area at the start of the working cycle, resulting in a high choking effect, maximum chamber pressure is not established instantaneously, but builds up gradually as the rotor turns. The pressure difference between the entry pressure p_E and the chamber pressure p_C is characteristic for the charging phase. This pressure difference results on the one hand from choking losses during inflow and on the other hand from gap mass flows. A further characteristic of the real charging procedure is the start of expansion before the high pressure side control edge is reached. The pressure gradient at chamber volume V_{Ex} already resembles that at of the first expansion phase as the control edge is reached from $V_{Ex,th}$. on. The reason for the early start of real expansion is mainly the combination of continually rising chamber volume and reduction in the area of the inlet opening towards the end of the charging phase. This early start is an inherent part of the system and it also occurs in an ideal simulation, ignoring choking and gap loss factors which result from flow obstruction in the inlet cross-section.

At the start of the expansion phase the operating behaviour of the screw motor is significantly influenced by the gap mass flows. In order to evaluate the influence of these flows on the energy conversion efficiency of the motor, we need to distinguish between mass flows out of the working chamber under examination and flows into it via the gap connections. Compared with isentropic expansion, the real pressure gradient during expansion is steeper at the theoretical start of expansion. The reason for this is the predominant share of mass flows out of the working chamber compared with flows into it. As the rotation angle increases, real and isentropic chamber pressures continue to converge, until, in the second phase of expansion, pressures for the real process attain higher values than those in the isentropic expansion phase. The flatter pressure curve of the real process in this area is a result of mass flows into the working chamber from the following chambers. These flows do not go direct to the low pressure side of the motor, but flow in part to the expanding chamber under examination, so that they apply work to the rotor flanks. The expansion phase ends when maximum chamber volume is attained. As a rule, at this rotation angle, the front tooth flanks cross the low pressure side control edges, and pressure equalisation takes place between the working fluid and the low pressure side volume (shown isochorically in Fig. 1). In the following, in order to represent the expulsion process, an idealised isochoric pressure equalisation process between the chamber pressure and the low pressure side ambient installation pressure is assumed. The influence of the pressure difference between the end of expansion and ambient back pressure is considered below, during examination of the internal volume ratios, in connection with “over and under-expansion”.

3. Performance data for the evaluation of screw motors

In order to evaluate the energy conversion efficiency of screw motors with varying geometrical parameters, performance figures and boundary conditions have to be laid down, at values for which the various different motors are comparable. Although a screw motor functions in basically the same way as a screw compressor rotating the opposite direction, both the definition of the boundary conditions and the physical description of the processes in the working chambers are more complex than in the case of screw compressors. In the following, performance figures will be defined and applied which permit both the assessment of differing rotor geometries, and the energy-based consideration of differing motor variants.

For a quantitative assessment of the gap situation and the configuration of the inlet area, the gap and inlet area operating data will be defined below. In contrast to flow rate and volumetric efficiency, the two previous sets of figures describe the geometric characteristics of the screw motor, and are independent of an energy-based examination of the whole working cycle.

The gap operating data relate the fluid mass $m_{G,fill}$ to the theoretical fluid mass $m_{Ex,th}$ at the start of expansion:

$$\Pi_G = \frac{m_{G,fill}}{m_{Ex,th}} \qquad \text{(Equation 1)}$$

The fluid mass $m_{G,fill}$ is the mass which, in the rotation angle area for charging between $\alpha_{fillbegin}$ and $\alpha_{Ex,th}$, flows out of the working chamber through the time-dependent gap area of the chamber to be charged A_G (t). For the gap flow, a supercritical decompression, reaching the speed of sound in the narrowest cross-section, is assumed

$$\Pi_G = \frac{\int_{\alpha_{fillbegin}}^{\alpha_{Ex,th}} A_G(t)\ \frac{1}{\omega}\,d\alpha \cdot \left(\frac{2}{\kappa_E+1}\right)^{\frac{1}{\kappa_E-1}} \cdot \frac{p_E}{R \cdot T_E}\sqrt{\frac{2 \cdot \kappa_E}{\kappa_E+1} \cdot R \cdot T_E}}{V_{Ex,th} \cdot \rho_E} \qquad \text{(Equation 2)}$$

The calculation is based on the model of a constant and isentropic gap flow through the narrowest cross-section, with negligible flow speeds before the entrance. If we assume that there is a flow blockage, the leakage becomes a function of the entry parameters (temperature and pressure), and the time (r.p.m.), and of the geometrical and time-dependent gap area. The theoretical mass can be computed from the chamber volume at the theoretical start of expansion, and the entry compression. It therefore depends on the entry parameters and the geometry of the screw motor.

The entry area operating data relates the mean fictive inflow speed to the speed of sound $a_E = f(p_E, T_E)$:

$$\Pi_{IA} = \frac{\bar{c}_{E,f}}{a_E} = \frac{\overline{\left(\frac{\dot{V}_C(t)}{A_{IA}(t)}\right)}}{a_E} \qquad \text{(Equation 3)}$$

The fictive inflow speed already used by Huster and Kauder is computed on the basis of the change in the chamber volume $\dot{V}_C(t)$ over time, and the inlet area A_{IA} (t). This means that the relationship between the mean fictive inflow speed and the speed of sound can be interpreted as a kind of mean fictive Mach number in the entry cross-section. Analogous to the gap operating data, the entry area data is only dependent on the geometry and the entry parameters. A motor with low entry area values is desirable, as this corresponds with a long charging phase and a large entry area.

4. Boundary conditions

In the following variation calculations, the parameter combination of entry pressure p_E and entry temperature ϑ_E are set as fixed boundary conditions for the screw motor, along with the mass flow at a constant ambient back pressure of $p_B = 10^5$ Pa. Although the variation options cover a broad, technically reasonable range, the fixing of the boundary conditions is not random, but is based on installation conditions of the type which occur in industrial applications with low mass flows.

- working medium: steam
- entry pressure $p_E = 7 \cdot 10^5$ Pa
- entry temperature $\vartheta_E = 350$ °C
- mass flow = 0,1 $kg \cdot s^{-1}$

In the following variation calculations, the mass flow is considered both as a theoretical reference value and as a real flow rate. The theoretical mass flow depends only on the machine geometry and the rotor speed, but not on the motor performance values, and is calculated via the following equation:

$$\dot{m}_{th} = V_{Ex,th} \cdot \rho_E \cdot z_{MR} \cdot n_{MR} = \frac{V_{max}}{v_i} \cdot \rho(p_E, T_E) \cdot z_{MR} \cdot n_{MR} \qquad \text{(Equation 4)}$$

The mass flow of the installation corresponds to the mass flow actually transported, and it depends not only on the machine geometry and the entry condition, but also on physical loss mechanisms. Along with the constant installation parameters, a number of other boundary conditions also need to be defined. These boundary conditions are laid down as the circumferential velocity at the tip circle of the rotors, and the mean gap height. For the variation in the rotor geometry, the male rotor circumferential velocity is set at u_{MR} = 80 m·s^{-1} as a constant. Gap heights of h_G = 0,1 mm for the entire machine are adopted as a constant.

5. Modelling and computing

The variation calculations were carried out in two independent computation steps: a geometrical abstraction and an energy-based examination. The basis of the geometrical abstraction of a screw motor is the analytical treatment of the rotor meshing. The objective of this calculation is to determine the volume curve, and to determine the inlet and outlet areas and the gap areas as a function of the male rotor angle, with preset geometrical parameters (z_{MR}, z_{MR}, φ_{MR}, L/D und v_i). The results of the geometrical abstraction are the basis for an energy-based examination of the operating behaviour of the motor.

The computing program for the energy-based machine analysis is based mainly on mass and energy conservation. Basically, by means of a balancing process, changes in the condition of the vaporous working fluid are ascertained numerically, so that the operating behaviour of the machine can be represented. This allows changes in condition in the form of rotation angle dependent volume changes, and gap mass flows in and out of the working chamber, to be taken into account. The computational basis for process changes in the working fluid is represented with reference to the flow velocity by a zero-dimensional chamber model, which permits, in principle, the simulation of screw motors with any range of geometrical parameters.

6. Geometrical variations

The following design for the geometrical parameters of the screw motor comprises variation in the internal volume ratios, the wrap angles, and the length-diameter ratios. As a starting point for the variation calculations, a tooth count combination of four male rotor teeth (z_{MR} = 4) and six female rotor teeth (z_{MR} = 6) was selected, which represents a compromise between low integral gap areas and a sufficiently large rotation angle area for chamber charging.

6.1. Variation of the internal volume ratio

The internal volume ratio is independent of the rotor geometry, and is configured exclusively via the position of the control edges in the motor housing. According to the official definition, the internal volume ratio of a screw motor is the result of the relationship between the maximum chamber volume at the end of expansion V_{max} and the chamber volume at the theoretical start of expansion $V_{Ex,th}$:

$$v_i = \frac{V_{max}}{V_{Ex,th}} \qquad \text{(Equation 5)}$$

Variation of the internal volume ratio of a screw machine takes place, in the case of deployment as a motor, by adjusting the position of the high pressure side control edges. With constant geometric rotor parameters, an increase in the internal volume ratio causes an adjustment of the control edges towards smaller rotor rotation angles, which results in a decrease in chamber volume at the start of expansion. Therefore, when varying the internal volume ratio, a requirement for constant mass flow in combination with constant male rotor circumferential velocity constitutes a significant restriction in machine dimensions.

The geometrical and energy-based effects of a variation in the internal volume ratio for machines with a wrap angle φ_{MR} = 300° and a length-diameter ratio L/D = 1,4 are illustrated below (**Fig. 2** and **Fig. 3**).

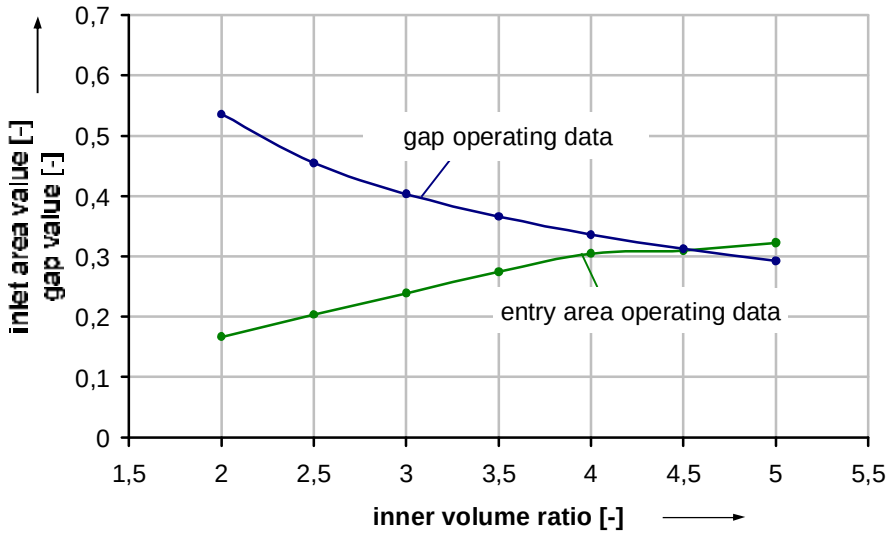

Fig 2: Entry area operating data and gap operating data as a function of the internal volume ratio for constant mass flow in the machine.

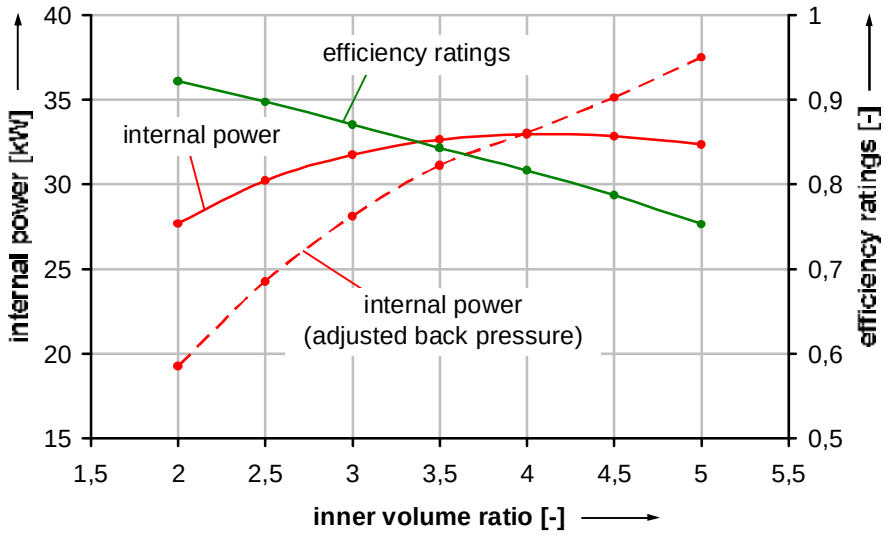

Fig 3: Internal isentropic efficiency rating and internal power at constant ambient back pressure and adapted operation as a function of the internal volume ratio.

At low internal volume ratios, the gap operating figures achieve maximum values, and the inlet area figures achieve minimal values. In this parameter area, the favourable inlet area data can be explained in terms of late arrival of the high pressure side control edge and the correspondingly large rotation angle area which is available for charging the working chamber, along with a large maximum inlet area. However, both the long charging time and the unfavourable gap situation lead to high mass flows through the gaps.

As internal volume ratios increase, the gap operating figures decrease and the inlet figures increase, which results mainly from the shorter rotation angle area available for the charging process. The dominant influence of inlet choking on the energy conversion efficiency of screw machines can be explained in terms of the dependence of the internal isentropic efficiency rating[2)] on the internal volume ratio. The efficiency rating drops virtually in a straight line as the internal volume ratio rises, in spite of an improving gap situation, as a consequence of the deteriorating charging situation . On the other hand, internal power is affected primarily by the relationship between chamber pressure at the end of expansion and ambient back pressure. If the internal volume ratio selected is too low, this leads to chamber pressure above the low pressure side ambient pressure, and this ‘under-expansion’ results in an idealised isochoric ‘after-expansion’ of the working fluid as the low pressure control edges are passed. Part of the theoretically available exergy of the fluid thus remains unused because the expansion phase is too short. Maximum internal power is produced in ‘adapted operation’. In this case there is no difference between the chamber pressure at the end of expansion and the low pressure side ambient pressure. As internal volume ratios continue to rise, chamber pressure drops below ambient pressure during expansion, and internal power falls away sharply. The ‘over-expanded’ fluid

[2)] The internal isentropic efficiency rating corresponds to the working area ratio of the loss-impaired motor when compared with the geometrically similar motor without losses (isobaric charging up to $V_{ex,th}$ and isentropic expansion up to V_{max}

mass is compressed in idealised isochoric form by the working fluid flowing back from the low pressure port before it is expelled. As soon as the chamber pressure falls below ambient pressure on the low pressure side, the effective work produced during the expansion of the fluid is over-compensated for by the work necessary for expulsion.

Fig. 3 shows the dependence of the internal power on the internal volume ratio for adjusted low pressure side back pressure. As examined here, the steam-powered screw motor always works in adjusted mode, and shows increasing internal power across the whole parameter range. This is a consequence of the increasing working area as the internal volume ratio rises, but it also shows – through the declining dependence of internal power on the internal volume ratio – the influence of the unfavourable inlet area situation with large internal volume ratios. An examination of the influence of the internal volume ratio on the thermodynamic operating behaviour of steam-powered screw motor reveals similar tendencies both for the mass flow in the installation and the theoretical mass flow as a design criterion. It was decided not to include the calculation results for machines with constant theoretical mass flows, as for this design boundary condition, tool, steam screw machines with an internal volume ratio which permits adjusted operation achieve the highest internal power results.

6.2. Variation of the wrap angle

In order to examine and evaluate the effects of varying the wrap angle on the energy conversion efficiency of screw motors, both for the design criterion of constant theoretical mass flow and for constant installation mass flow, a number of pairs of rotors are varied so that only the wrap angle changes. The length-diameter ratios and the internal volume ratios of all rotor pairs remain constant. Varying the wrap angle influences both the gap situation and the geometry of the inlet area. For the quantitative description of the geometrical effects of the machine variations, an entry area value Π_{IA} and a gap value Π_G are used. The dependence of both values and that of the volumetric efficiency on the wrap angle, plus the internal power and the internal isentropic efficiency rating as a function of the wrap angle, are represented in **Fig. 4** and **Fig. 5** for screw motors with an internal volume ratio of $v_i = 3,5$ and a length-diameter ratio L/D = 1,4, for the design criterion of constant theoretical mass flow.

The geometry of motor variants with small wrap angles is characterised by a favourable gap situation and unfavourable inlet area geometry. For these motor variants both the internal isentropic efficiency rating and the internal power rating only attain minimal values. As the wrap angle increases, the efficiency rating and the internal power rise digressively, which can be explained in terms of integrally reducing dissipation. With reference to the entry area and gap operating datas, the most important factor is the improved energy conversion efficiency which is brought about by better inlet geometry as a result of increasing wrap angles. This factor plays a greater role than the deteriorating gap situation. If we consider the design criterion of constant theoretical mass flow, the favourable characteristics, from an energy conversion point of view, of motors with large wrap angles, are present for all length-diameter ratios and internal volume ratios examined. The volumetric efficiency of the steam-powered screw motors under examination rises as the wrap angle increases from $\lambda_L \approx 0,95$ to $\lambda_L \approx 1,2$ upwards.

Concerning constant installation conditions, machine versions with large wrap angles show a corresponding installation mass flow, which lies about 20 % above the theoretical mass flow set as a design criterion.

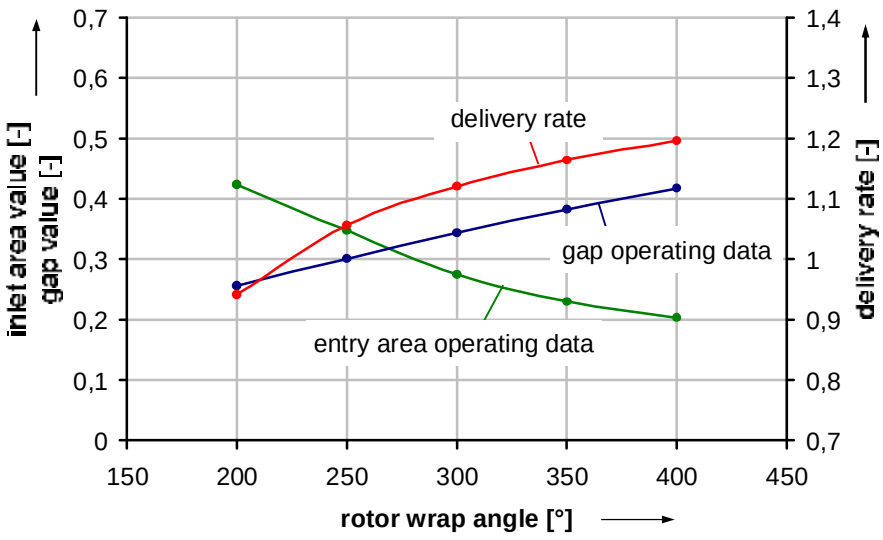

Fig. 4: Entry area operating data, gap operating datas and delivery rate as a function of the wrap angle for constant theoretical mass flow

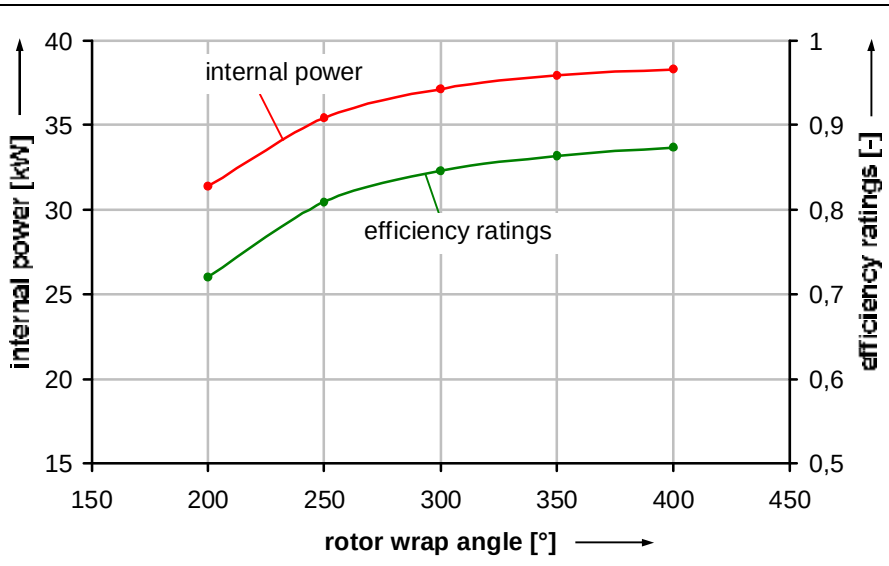

Fig. 5: Internal isentropic efficiency rating and internal power as a function of the wrap angle for constant theoretical mass flow

The effects of geometrical scaling of the motors on a constant installation mass flow are outlined in **Fig. 6** and **Fig. 7** for the machine parameters already utilised.

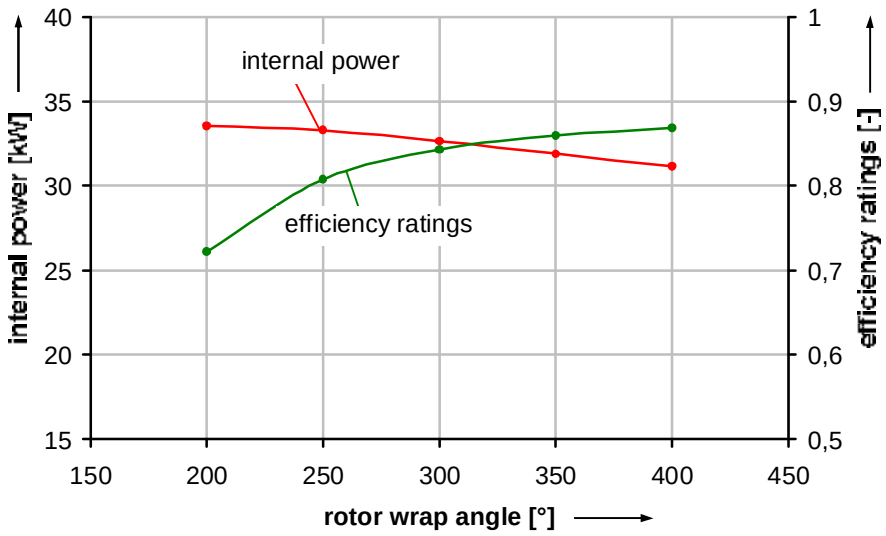

Fig. 6: Internal isentropic efficiency rating and internal power as a function of the wrap angle for constant installation mass flow

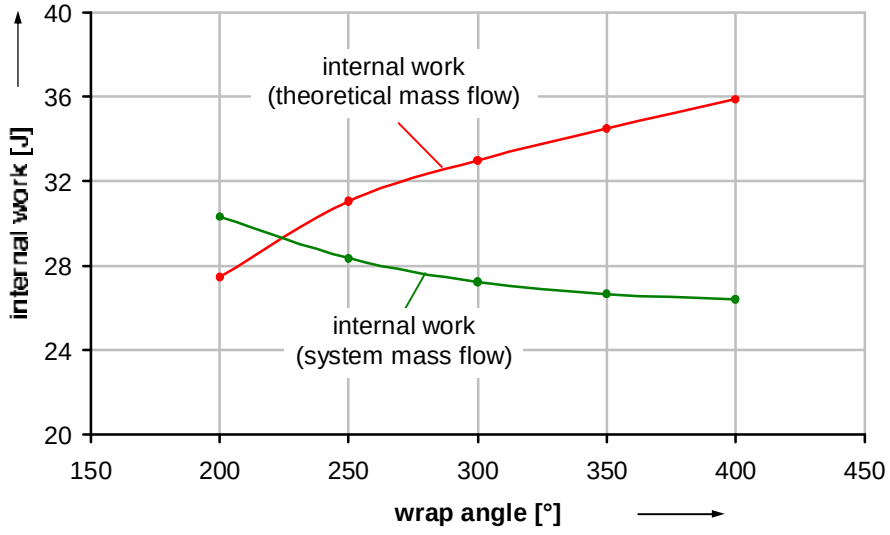

Fig. 7: Internal work for constant theoretical and system mass flow as a function of the wrap angle

While for a configuration based on theoretical mass flow the largest possible wrap angle emerges as reasonable from an energy point of view, constant installation mass flow machines with small wrap

angles produce the highest internal power. Although, as the qualitative interrelation of the geometric performance data (not covered here) and the internal isentropic efficiency remain unchanged, this state of affairs appears paradoxical, this shift in the internal power data can be explained via the scaling of the machine. In the large wrap angle area, the geometrical reduction in the size of the machine, a consequence of scaling down, results in a reduction in chamber volume. The energy-based influence of the reduction in volume is clarified by a computation of the internal work by means of the closed ring integral $W_i = \oint pdV$ and accordingly the internal power $P_i = \oint pdV \cdot z_{MR} \cdot n$. The reduction in the working area for motors with a large wrap angle is mainly responsible for the lower internal power at constant installation mass flows. The influence of rotor speed changes on internal power, also caused by scaling, is limited compared with the contribution to internal work. As far as constant installation parameters are concerned, it would appear that advocating large wrap angles, which would be the consequence of setting constant theoretical mass flow as a criterion, is not to be recommended.

6.3. Varying the length-diameter ratio

Along with the tooth count and the wrap angle, the length-diameter ratio is the third parameter which describes the rotor geometry. The variation area discussed below covers the range from length-diameter ratios L/D = 1,0 – 2,0. Analogous to the wrap angle, the length-diameter ratio influences both the total gap situation and the geometry of the inlet area of a steam-powered screw motor.

In **Fig. 8** and **Fig. 9**, for the design criterion of constant theoretical mass flow, both geometrical values, volumetric efficiency, the internal isentropic efficiency rating and internal power for an internal volume ratio of $v_i = 3,5$ and a wrap angle of $\varphi = 300°$ are represented.

In the area of small length-diameter ratios, the gap operating datas attain maximum ratings, and the entry area operating datas attain minimum ratings. As the length-diameter ratio increases, the growing entry area operating data is responsible for deteriorating geometrical characteristics in that area, while the reducing gap operating data exercises a positive influence on the gap situation. The effects of a rising length-diameter ratio on the inlet situation are qualitatively comparable with the influence of a reducing wrap angle at constant theoretical mass flow. Both the maximum value of the inlet area and the charging times decline as the length-diameter ratio falls, and are responsible for the high entry area operating datas in this parameter area. On the other hand, the reduced charging times have a favourable effect on the gap operating datas. As the length-diameter ratio increases, charging times and decreasing integral gap areas also contribute to the decline in this value. Both the internal isentropic efficiency rating and internal power attain maximum values at low length-diameter ratios, which, analogous to varying the wrap angle at constant theoretical mass flow, can be attributed to the predominant role of choking losses during charging compared with gap losses. The differences in volumetric efficiency from $\lambda_L \approx 1,18$ at small length-diameter ratios to $\lambda_L \approx 1,09$ at large length-diameter ratios are much smaller than is the case with wrap angle variation. Accordingly, scaling at

constant installation mass flow results in downsizing the machine across the entire parameter range under consideration. Machines with a small length-diameter ratio are the most seriously affected.

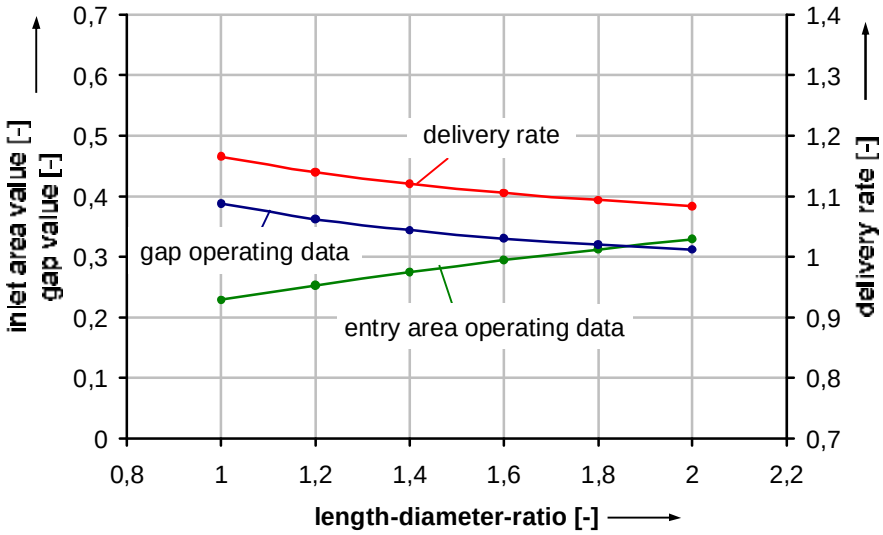

Fig. 8: Entry area operating data, gap operating data and delivery rate as a function of the length-diameter ratio for constant theoretical mass flow

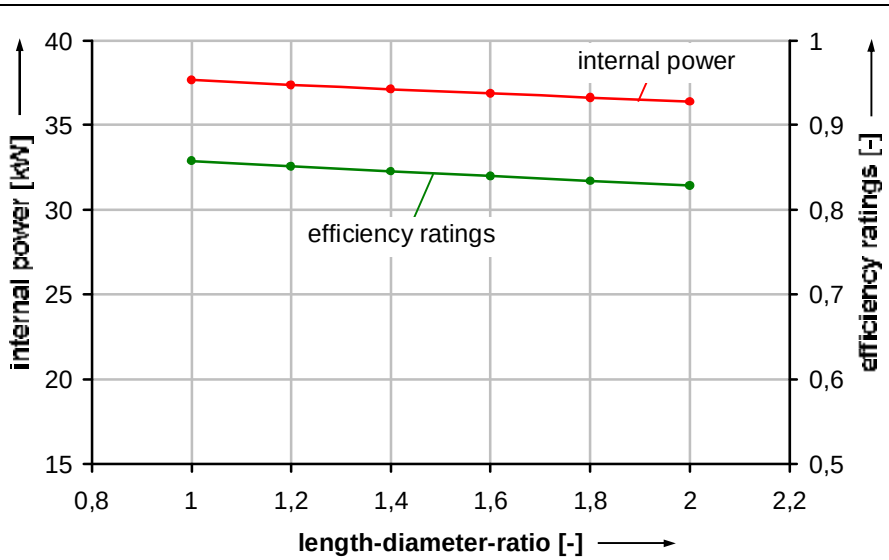

Fig. 9: Internal isentropic efficiency rating and internal power as a function of the length-diameter ration for constant theoretical mass flow

The energy figures for the scaled machines are represented in **Fig. 10** and **Fig. 11** as a function of the length-diameter ratio. As has been established for wrap angle variation, for length-diameter ratios, too,

scaling under constant installation conditions has no qualitative effect on geometrical performance values or isentropic efficiency rating.

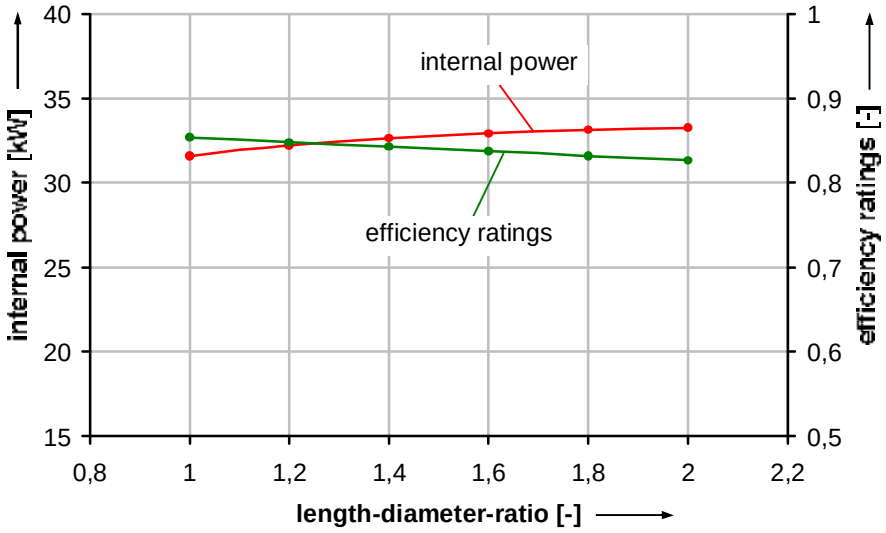

Fig. 10: Internal isentropic efficiency rating and internal power as a function of the length-diameter for constant installation mass flow

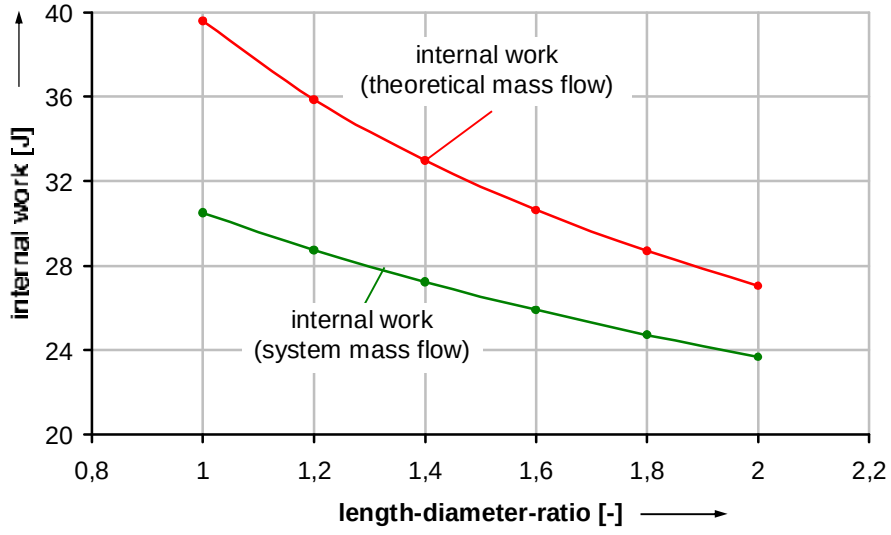

Fig. 11: Internal work as a function of the length-diameter ration for constant installation mass flow and theoretical mass flow

Scaling down entails a decrease in internal work across the whole range of variation. This decrease is most obvious in the case of small length-diameter ratios for machines with high volumetric efficiency.

However, internal work continues to attain maximum values at small length-diameter ratios. The rise in internal power as length-diameter ratios increase can not therefore be attributed to the enclosed working area of the thermodynamic cycle. It depends rather on the rise in rotor speed as a consequence of decreasing rotor diameter at high length-diameter ratios. While rotor speed changes played a minor role when the wrap angle was varied, for the machine examined in Fig. 10 and Fig. 11, across the range from n(L/D = 1,0) = 259 s^{-1} to n(L/D = 2,0) = 351 s^{-1} there was an increase of 35,5 % in rotor speed effect as the length-diameter ratio was varied. This explains the high internal power in the case of large length-diameter ratios.

For the used boundary conditions, the geometric parameters of the steam-powered screw motor are set to an internal volume ratio vi = 3,8, a wrap angle φ_{MR} = 300° and a length-diameter ratio L/D = 1,4. The chosen values are in case of the internal volume ratio and the wrap angle just a matter of the energetic analyses. The selected length-diameter ratio is a compromise between appropriate available space for bearings and packings on the one hand and good internal power on the other hand.

[1] Kliem, B.: Die Expansion von Naßdampf in Schraubenmotoren zur Nutzung von Abwärme - Ein Beitrag zur Auslegung von Zweiphasenschraubenmotoren. Dissertation, TU - Dortmund (2004)

[2] von Unwerth, T.: Experimentelle Verifikation eines Simulationssystems für eine GASSCREW. Dissertation, TU – Dortmund, (2002)

[3] Zellermann, R.: Optimierung von Schraubenmotoren mit Flüssigkeitseinspritzung. Dissertation, TU – Dortmund, (1996)

[4] Fost, C.: Ein Beitrag zur Verbesserung der Kammerfüllung von Schraubenmotoren. Dissertation, TU – Dortmund, (2003)

[5] Huster, A.: Untersuchung des instationären Füllvorgangs bei Schraubenmotoren. Dissertation, TU – Dortmund, (1998)

Symbol	Dimension	Meaning
a	$m\ s^{-1}$	speed of sound
A	m^2	Area
c	$m\ s^{-1}$	flow speed
D	M	diameter
h	M	gap height
l	M	length
$\dot{m}$	$Kg\ s^{-1}$	mass flow
n	s^{-1}	r.p.m
p	Pa	pressure
P	W	power/performance
R	$J\ kg^{-1}\ K^{-1}$	gas constant
t	S	time
T	K	temperature
u	$m\ s^{-1}$	rim speed
V	m^3	volume
$\dot{V}$	$m^3\ s^{-1}$	volume flow
W	$Kg\ m^2\ s^{-2}$	work, working area
v_i	-	internal volume ratio
z	-	tooth count

Symbol	Dimension	Meaning
°	Grad	rotation angle
η	-	efficiency rating
κ	-	isentropic exponent
Π_{IA}	-	entry area operating
Π_G	-	gap operating data
ρ	$kg\ m^{-3}$	density
φ	Grad	wrap angle
ϑ	°C	degrees Celsius

Symbol	Meaning
B	back pressure
C	chamber
E	entry/inlet
IA	inlet area
Ex	start of expansion
Ex,th	theoretical start of expansion
F	fictional
fill	charging
fillbegin	begin of filling / charging
Id	ideal
G	gap/clearance